

Virtual quantum error detection

Kento Tsubouchi,^{1,*} Yasunari Suzuki,² Yuuki Tokunaga,² Nobuyuki Yoshioka,^{1,3,4} and Suguru Endo^{2,†}

¹*Department of Applied Physics, University of Tokyo,
7-3-1 Hongo, Bunkyo-ku, Tokyo 113-8656, Japan*

²*NTT Computer and Data Science Laboratories,
NTT Corporation, Musashino, 180-8585, Tokyo, Japan*

³*Theoretical Quantum Physics Laboratory, RIKEN Cluster for Pioneering Research (CPR), Wako-shi, Saitama 351-0198, Japan*

⁴*JST, PRESTO, 4-1-8 Honcho, Kawaguchi, Saitama, 332-0012, Japan*

Quantum error correction and quantum error detection necessitate syndrome measurements to detect errors. Syndrome measurements need to be performed for each stabilizer generator with single-shot measurements, which can be a significant overhead, considering the fact that the readout fidelity is generally lower than gate fidelity in the current quantum hardware. Here, by generalizing a quantum error mitigation method called symmetry expansion, we propose a protocol that we call virtual quantum error detection (VQED). This method *virtually* allows for evaluating computation results corresponding to post-selected quantum states obtained through quantum error detection during circuit execution without syndrome measurements. Furthermore, while the conventional quantum error detection needs the implementation of Hadamard test circuits for each stabilizer generator, our VQED protocol can be performed with a constant depth shallow quantum circuit with an ancilla qubit, irrespective of the number of stabilizer generators. In addition, VQED is fully compatible with other error mitigation schemes for further improvement of computation accuracy, thus leading to high-fidelity quantum computing.

I. INTRODUCTION

The last decade has seen the remarkable development of the noisy-intermediate quantum computing paradigm from both theoretical and experimental sides [1–8]. Nevertheless, the effect of noise lies as a crucial problem in realizing practical quantum computing. Quantum error correction (QEC) and quantum error detection (QED), which reduce computation errors through the encoding of logical qubits with many physical qubits, have been investigated for enhancing computation accuracy for a long time since the early days of quantum information science [9–14]. Syndrome measurements to detect physical errors by using ancilla qubits are performed in QEC and QED; QEC actively corrects physical errors based on the error information obtained in the decoding process while QED discards the noisy quantum states once an error is detected.

While the utility of QEC and QED have been shown theoretically in numerous previous works, they require high-fidelity syndrome measurements of stabilizer generators. Furthermore, the number of required syndrome measurements increases as the number with that of stabilizer generators of the QEC/QED code. Considering the current situation of superconducting hardware, in which the measurement fidelity is lower than gate errors [6, 15, 16], the necessity of single-shot measurements for syndrome measurements can be a significant overhead in QEC/QED.

For the ease of error reduction in near-term quantum hardware, a class of error reduction techniques re-

ferred to as quantum error mitigation (QEM) has been recently studied [17–21]. In many QEM methods, the noiseless expectation values of observables are estimated via post-processing of measurement results. This indicates that we cannot physically obtain error-mitigated quantum states but QEM only *virtually* simulates them only for expectation values. Symmetry expansion (SE) is one of the QEM methods that use symmetries inherent to the system for error mitigation [22–25]. The noisy quantum state is virtually projected onto the symmetric subspace by random sampling of the symmetry operators, additional measurements, and classical postprocessing of measurement outcomes. As we will discuss later, SE allows for the calculation of the expectation value of an observable corresponding to the post-selected quantum states through QED without implementing syndrome measurements, and hence is suitable for near-term hardware. So far, SE is theoretically formulated for error mitigation for noisy states immediately before measurement [23, 24] and state preparation for rotation symmetric bosonic codes [25], whereas the conventional QED can be more flexibly used during the circuit execution.

In this work, we significantly expand the framework of SE so that it can be leveraged during the execution of quantum algorithms. Because our method enables us to obtain the expectation values corresponding to the post-selected state via QED, we call it *virtual quantum error detection* (VQED). Although VQED inherits the disadvantages of SE, i.e., we can only obtain error-mitigated expectation values, not the quantum state itself, and the required sampling complexity is quadratically worse for the success probability of QED, the significant advantages of VQED compared with the QED are as follows: 1. the depth for QEM is constant regardless of the number of stabilizer generators of the code; 2. we only measure

* tsubouchi@noneq.t.u-tokyo.ac.jp

† suguru.endo@hco.ntt.co.jp

an expectation value of an observable without the need for single-shot syndrome measurements; 3. our method is fully compatible with other QEM methods, e.g., readout error mitigation for the ancilla qubit used in our protocol. We numerically verify the behavior of the fidelity improvement with our VQED protocol over the conventional SE and the unencoded cases and evaluate the required sampling costs. We also remark that our method can offer virtual implementation of stabilizer-like QEM methods using spin and particle number preservation in the computation [22, 26] in even more hardware-friendly manner.

In addition, we discuss the virtual implementation of quantum error correction, which results in the computation outcome corresponding to the error-corrected quantum states. While the conventional QEC does not induce additional sampling overheads, we find that our virtual QEC generally incurs a larger sampling overhead than the virtual QED method; therefore, we conclude VQED is preferred in typical quantum computation scenarios.

II. PRELIMINARIES

A. Quantum error detection and quantum error correction for stabilizer codes

We first review stabilizer codes and ways to detect and correct their errors [27, 28]. QED and QEC are performed by encoding quantum information into enlarged Hilbert space at the expense of multiple quantum systems. Due to its redundancy, we can detect and correct their errors during the computation.

Here, we review the stabilizer formalism, which is the most standard method to construct quantum error-correcting codes. Consider an n -qubit Pauli group as

$$\mathcal{G}_n = \{\pm 1, \pm i\} \times \{I, X, Y, Z\}^{\otimes n} \quad (1)$$

where I is the identity operator for single qubit system and $X = \begin{pmatrix} 0 & 1 \\ 1 & 0 \end{pmatrix}$, $Y = \begin{pmatrix} 0 & -i \\ i & 0 \end{pmatrix}$, and $Z = \begin{pmatrix} 1 & 0 \\ 0 & -1 \end{pmatrix}$ are Pauli operators. To encode k logical qubits into n physical qubits, we define a stabilizer group $\mathcal{S} = \{S_1, \dots, S_{2^{n-k}}\} \subset \mathcal{G}_n$ as a commutative subgroup of the Pauli group \mathcal{G}_n with $-I^{\otimes n} \notin \mathcal{S}$. We denote a generator set of the stabilizer group \mathcal{S} as $\mathcal{G} = \{G_1, \dots, G_{n-k}\}$. Then, we can define the logical space of the stabilizer code \mathcal{C} as an eigenspace with +1 eigenvalues for all the operators in the stabilizer group, i.e., $\mathcal{C} = \{|\psi\rangle \mid \forall S_i \in \mathcal{S}, S_i |\psi\rangle = |\psi\rangle\}$. In the 2^k -dimensional Hilbert space, we can introduce a logical basis as $\{|0\rangle_L, |1\rangle_L\}^{\otimes k}$ and logical Pauli operators as $\{I_L, X_L, Y_L, Z_L\}^{\otimes k}$. The code distance d is the minimum number of physical qubits on which an arbitrary logical operator of the code non-trivially operates. We denote such stabilizer codes as $[[n, k, d]]$ stabilizer codes.

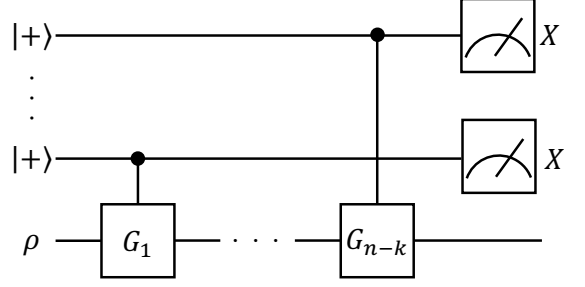


FIG. 1. Quantum circuit for quantum error detection (QED).

We can detect physical errors during quantum computation by measuring the generators G_1, \dots, G_{n-k} by using the Hadamard test circuits as shown in Fig 1, which is called syndrome measurement. If there exists G_i such that its measurement result is -1 , then we can determine the presence of errors during the computation. Conversely, when the measurement results are $+1$ for all G_i , we can say that there was no error with a sufficiently high probability. By continuing the computation only when the measurement results for all the generators are $+1$, we can project the noisy state $\rho = \mathcal{E}(\rho_{\text{id}})$ into the code space as

$$\rho_{\text{det}} = \frac{P\rho P}{\text{tr}[\rho P]}, \quad (2)$$

where P is an projector to the code space \mathcal{C} written as

$$P = \prod_{G_i \in \mathcal{G}} \frac{I + G_i}{2} = \frac{1}{2^{n-k}} \sum_{S_i \in \mathcal{S}} S_i. \quad (3)$$

Because the probability to measure $+1$ for all the syndrome measurements is $\text{tr}[\rho P]$, the effect of physical errors acting on less than d qubits can be eliminated with $O(\text{tr}[\rho P]^{-1})$ times more execution of quantum circuits. Note that stabilizer-like QEM methods work in a similar way when the spin and electron number preservation is imposed in the variational ansatz of quantum states [22, 26].

We can not only detect errors but also correct them by applying appropriate feedback operations according to the measurement results, enabling us to suppress the effect of noise without any additional execution of quantum circuits. When the measurement result for the generator G_i is s_i , and there is no measurement error, we can correct errors by applying a recovery operation R_s , which is estimated from $s = (s_1, \dots, s_{n-k})$ to maximize the probability of correcting erroneous quantum states to the original logical state. Since the recovery Pauli operator at least maps quantum states to a logical state, R_s commutes with G_i if $s_i = +1$ and anti-commutes if $s_i = -1$. In this way, the effect of physical errors acting on less than $\lfloor (d-1)/2 \rfloor$ qubits can be corrected as

$$\rho_{\text{cor}} = \sum_{s \in \{-1, 1\}^{n-k}} E_s \rho E_s, \quad (4)$$

where

$$\begin{aligned} E_s &= R_s \prod_i \frac{I + s_i G_i}{2} \\ &= P R_s. \end{aligned} \quad (5)$$

While QEC and QED can reduce the effective error rates, they impose additional difficulties in the implementation. To implement QEC and QED, we need repetitive applications of Pauli measurements for all the elements in the stabilizer generator set. Since the error rates of measurement operations are typically higher than the others [6, 15, 16], they induce large overheads on the process. In the case of QEC, we also need to estimate recovery operations from the observed syndrome values, and error rates must be smaller than the value called code threshold for a reliable estimation.

B. Symmetry expansion

In order to combat errors on near-term devices, QEM has been developed in recent years [20, 21]. Symmetry expansion (SE) is one of the promising QEM methods which mitigates errors by virtually projecting the noisy quantum state onto the symmetric subspace without syndrome measurements [23, 24].

Suppose that we want to estimate an expectation value of an observable O for a noiseless state ρ_{id} from the measurement of the noisy state $\rho = \mathcal{E}(\rho_{\text{id}})$. We assume that the observable O commutes with the projector P . Then, we can mitigate errors by virtually projecting the noisy states onto the code space as

$$\begin{aligned} \text{tr}[\rho_{\text{det}} O] &= \frac{\text{tr}[\rho O P]}{\text{tr}[\rho P]} \\ &= \frac{2^{-(n-k)} \sum_{S_i \in \mathcal{S}_i} \text{tr}[\rho O S_i]}{2^{-(n-k)} \sum_{S_i \in \mathcal{S}_i} \text{tr}[\rho S_i]}, \end{aligned} \quad (6)$$

which can be calculated in the following way.

1. For $s = 1, \dots, N$, repeat the following operations.

- (a) Uniformly sample $S_i \in \mathcal{S}$.
- (b) Simultaneously measure the noisy state ρ for S_i and $O S_i$ and record the results as a_s and b_s .

2. Calculate $a = \frac{1}{N} \sum_s a_s$ and $b = \frac{1}{N} \sum_s b_s$.

3. Output b/a .

The number of measurements needed to estimate Eq. (6) for some fixed accuracy ε is known to scale as $N = O(\varepsilon^{-2} \text{tr}[\rho P]^{-2})$. In this way, we can obtain an error-mitigated expectation value of the observable O , which corresponds to the virtual projection of the noisy state ρ onto ρ_{det} .

III. VIRTUAL QUANTUM ERROR DETECTION

Symmetry expansion is only applicable to the state immediately before measurement [23, 24] and state preparation for rotation symmetric bosonic codes [25]. In this section, we introduce our VQED method, which allows for the computation of error-mitigated expectation values corresponding to the post-selected states after syndrome measurements during circuit execution.

We consider a logical quantum circuit composed of a state preparation of a logical initial state ρ_0 followed by L logical unitary gate $\mathcal{U}_l(\cdot) = U_l \cdot U_l^\dagger$ ($l = 1, \dots, L$) and a measurement of an observable O in the hope of estimating the expectation value of O for the state $\rho_{\text{id}} = \mathcal{U}_L \circ \dots \circ \mathcal{U}_1(\rho_0)$. However, we assume that these logical quantum gates are affected by Markovian noise and that the actual gates are represented as $\mathcal{U}'_l = \mathcal{E}_l \circ \mathcal{U}_l$. For simplicity, we ignore state preparation and measurement (SPAM) errors, but these effects can easily be reflected. When we can perform quantum error detection after each gate, we will have

$$\rho_{\text{det}} = \frac{\rho'_{\text{det}}}{\text{tr}[\rho'_{\text{det}}]}, \quad (7)$$

where

$$\rho'_{\text{det}} = \mathcal{P} \circ \mathcal{E}_L \circ \mathcal{U}_L \circ \dots \circ \mathcal{P} \circ \mathcal{E}_1 \circ \mathcal{U}_1(\rho_0). \quad (8)$$

Here, we define $\mathcal{P}(\cdot) = P \cdot P$.

In order to obtain the expectation value for ρ_{det} through VQED, we construct a quantum circuit represented in Fig. 2. This circuit allows for computation of the expectation values corresponding to the error-detection circuits by preparing a single qubit ancilla initialized to $|+\rangle$, coupling the ancilla qubit with the noisy circuit through control- S_{i_l} for the state 0 and control- S_{j_l} gate for the state 1, and measuring the ancilla in the X bases. Note that the number of this operation for VQED can be reduced according to the noise level, although we discuss gate-wise VQED for generality. The state immediately before the measurement of this circuit ρ_{bf} reads:

$$\begin{aligned} \rho_{\text{bf}} &= \frac{1}{2^L} \sum_{\mathbf{p}\mathbf{q}} |\mathbf{p}\rangle \langle \mathbf{q}| \otimes \rho_{\mathbf{ij}}^{\mathbf{pq}}, \\ \rho_{\mathbf{ij}}^{\mathbf{pq}} &= \mathcal{P}_{i_L j_L}^{p_L q_L} \circ \mathcal{E}_L \circ \mathcal{U}_L \circ \dots \circ \mathcal{P}_{i_1 j_1}^{p_1 q_1} \circ \mathcal{E}_1 \circ \mathcal{U}_1(\rho_0), \end{aligned} \quad (9)$$

where \mathbf{p} and \mathbf{q} are bitstrings of length L and

$$\mathcal{P}_{i_l j_l}^{p_l q_l}(\cdot) = S_{j_l}^{p_l} S_{i_l}^{1-p_l} \cdot S_{i_l}^{1-q_l} S_{j_l}^{q_l}. \quad (10)$$

Then, the expectation value of the observable $X^{\otimes L} \otimes O$ in this state is:

$$\begin{aligned} \langle X^{\otimes L} \otimes O \rangle &= \text{tr}[\rho_{\text{bf}} X^{\otimes L} \otimes O] \\ &= \frac{1}{2^L} \sum_{\mathbf{p}} \text{tr}[\rho_{\mathbf{ij}}^{\mathbf{pp}+1} O] \end{aligned} \quad (11)$$

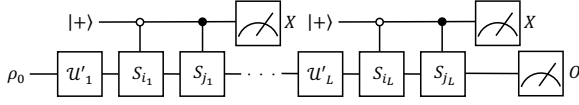


FIG. 2. Quantum circuit for virtual quantum error detection (VQED). The white/black circles indicate the control operations which act for the state 0/1.

where $\mathbf{1}$ is a bit string of length L whose elements are all 1. When we uniformly sample $i_l, j_l \in \{1, \dots, 2^{n-k}\}$ ($1 \leq l \leq L$) and denote the expectation value under the probability distribution as $\langle \cdot \rangle_{ij}$, we can project the noisy state into the code space after each noisy gate as

$$\langle \rho_{ij}^{pp+1} \rangle_{ij} = \mathcal{P} \circ \mathcal{E}_L \circ \mathcal{U}_L \circ \dots \circ \mathcal{P} \circ \mathcal{E}_1 \circ \mathcal{U}_1(\rho_0) \quad (12)$$

$$= \rho'_{\text{det}},$$

where we use

$$\begin{aligned} \langle \mathcal{P}_{ijl}^{p_l+1}(\cdot) \rangle_{ijl} &= \langle S_{j_l}^{p_l} S_{i_l}^{1-p_l} \cdot S_{i_l}^{p_l} S_{j_l}^{1-p_l} \rangle_{ijl} \\ &= \begin{cases} \langle S_{i_l} \cdot S_{j_l} \rangle_{ijl} & (p_l = 0) \\ \langle S_{j_l} \cdot S_{i_l} \rangle_{ijl} & (p_l = 1) \end{cases} \quad (13) \\ &= P \cdot P. \end{aligned}$$

Thus, The expectation value of the observable O for the post-selected state ρ_{det} can be represented as:

$$\text{tr}[\rho_{\text{det}} O] = \frac{\langle \text{tr} \left[\left(\frac{1}{2^L} \sum_{\mathbf{p}\mathbf{q}} |\mathbf{p}\rangle \langle \mathbf{q}| \otimes \rho_{ij}^{pq} \right) X^{\otimes L} \otimes O \right] \rangle_{ij}}{\langle \text{tr} \left[\left(\frac{1}{2^L} \sum_{\mathbf{p}\mathbf{q}} |\mathbf{p}\rangle \langle \mathbf{q}| \otimes \rho_{ij}^{pq} \right) X^{\otimes L} \otimes I \right] \rangle_{ij}}. \quad (14)$$

Therefore, we can perform our VQED in the noisy quantum circuit with the following procedure:

1. For $s = 1, \dots, N$, repeat the following operation.
 - (a) Uniformly sample $i_l, j_l \in \{1, \dots, 2^{n-k}\}$ ($1 \leq l \leq L$).
 - (b) Run the circuit illustrated in Fig. 2.
 - (c) Record the product of the X measurement as a_s and the product of a_s and O measurement as b_s .
2. Calculate $a = \frac{1}{N} \sum_s a_s$ and $b = \frac{1}{N} \sum_s b_s$.
3. Output b/a .

In this way, with the sampling overhead of $N = O(\varepsilon^{-2} \text{tr}[\rho'_{\text{det}}]^{-2})$, we can perform VQED in quantum circuits that occurred during the computation with some fixed accuracy ε . Note that while we focus on the stabilizer QEC/QED codes, our method can be straightforwardly applied to the stabilizer-based QEM method for the spin and electron number preservation [22, 26] for more near-term quantum hardware.

Note that our VQED protocol circumvents the syndrome measurements of stabilizer generators that need

high-fidelity single-shot measurement of ancilla qubits; our method only measures expectation values of the observable. Furthermore, while quantum error detection requires measurements of $n - k$ stabilizer generators via Hadamard test circuits shown in Fig. 1, our method only necessitates two-controlled operations irrespective of the number of stabilizer generators. Lastly, by combining the readout error mitigation method with our method for the ancilla qubit, we can perform high-fidelity virtual projection onto the code space even when we use noisy ancilla qubits. The disadvantages of VQED are that we can only obtain the error-mitigated expectation values, not the quantum state itself as well as quadratically worse sampling cost for the projection probability $\text{tr}[\rho'_{\text{det}}]$. While sampling costs can only be overcome by increased parallelization, lightweight quantum phase estimation algorithms only employing expectation values are proposed [29–32] in addition to the fact that most of NISQ algorithms use expectation values.

IV. VIRTUAL IMPLEMENTATION OF QUANTUM ERROR CORRECTION

We also discuss how to perform quantum error correction virtually without any syndrome measurements and feedback operations. The main idea is that the error-corrected state as in Eq. (4) can be also written as

$$\rho_{\text{cor}} = \sum_{\mathbf{s} \in \{-1, 1\}^{n-k}} \mathcal{P}(R_{\mathbf{s}} \rho R_{\mathbf{s}}). \quad (15)$$

Thus, we can virtually correct errors by uniformly sampling $s_1, \dots, s_{n-k} \in \{+1, -1\}$, applying $R_{\mathbf{s}}$ to the noisy state, virtually projecting the state into the codespace using the way mentioned above, and multiplying the result by 2^{n-k} . However, the sampling cost of this method scales as $2^{2(n-k)}$, which grows exponentially with the number of redundant circuits. We may decrease the cost by limiting the scope of the sum. Let $B \subset \{-1, 1\}^n$ be a subset of highly probable measurement results such as the measurement results when an error did not occur or occurred only once. Then, we may approximate the error-corrected state as

$$\rho_{\text{cor}'} = \frac{1}{\sum_{\mathbf{s} \in B} p_{\mathbf{s}}} \sum_{\mathbf{s} \in B} \mathcal{P}(R_{\mathbf{s}} \rho R_{\mathbf{s}}) \quad (16)$$

where $p_{\mathbf{s}} = \text{tr}[P R_{\mathbf{s}} \rho R_{\mathbf{s}}]$ represents the probability of obtaining \mathbf{s} at the syndrome measurement. However, the sampling cost of virtually calculating this state is $|B|^2 / (\sum_{\mathbf{s} \in B} p_{\mathbf{s}})^2$, which is still significantly higher than just performing VQED with $B = \{1\}^n$. Furthermore, while error detection can detect errors of at most d qubits, error correction can only correct errors of at most $\lfloor (d-1)/2 \rfloor$ qubits. This means that even the accuracy of this virtual implementation of QEC is generally worse than VQED. Even though these methods may be more effective than VQED in the case where the noise maps

(a) $[4, 1, 2]$ stabilizer code

Name	Operator
G_1	$XXXX$
G_2	$ZZZZ$
G_3	$IZZ I$
Z_L	$ZZII$
X_L	$IXXI$

(b) $[5, 1, 3]$ stabilizer code

Name	Operator
G_1	$XZZXI$
G_2	$IXZZX$
G_3	$XIXZZ$
G_4	$ZXIXZ$
Z_L	$ZZZZZ$
X_L	$XXXXX$

(c) $[7, 1, 3]$ stabilizer code

Name	Operator
G_1	$IIIZZZZ$
G_2	$IZZIIZZ$
G_3	$ZIZIZIZ$
G_1	$IIIXXXX$
G_2	$IXXIIXX$
G_3	$XIXIXIX$
Z_L	$ZZZZZZZ$
X_L	$XXXXXXX$

TABLE I. Generators and logical operators for (a) $[4, 1, 2]$, (b) $[5, 1, 3]$, and (c) $[7, 1, 3]$ stabilizer codes.

the state in the code space outside of it with high probability, finding practical scenarios to utilize these methods is left as our future work.

V. NUMERICAL SIMULATION

In this section, we numerically evaluate the performance of our method for $[4, 1, 2]$, $[5, 1, 3]$, and $[7, 1, 3]$ stabilizer codes [11, 12, 14]. The generators and logical operators of these codes are shown in Tabel I. We set the initial state ρ_0 to be the logical 0 state $|0\rangle_L$ and unitary gate as $U_l = e^{i\theta_l Z_L} e^{i\theta'_l X_L}$ where θ_l, θ'_l is uniformly sampled from $[0, 2\pi)$. We assume that the local depolarizing noise $\mathcal{E} = \mathcal{E}_p^{\otimes n}$ ($\mathcal{E}_p(\rho) = (1-p)\rho + \frac{p}{2}I$) disturb the circuit with noise strength $p = 0.01$ each after the gate. We numerically calculate the depth L dependence of the infidelity $1 - \langle \bar{\Psi} | \rho_{\text{det}} | \bar{\Psi} \rangle$ between the output state of the noisy circuit ρ_{det} and the noiseless circuit $|\bar{\Psi}\rangle$ and the scaling of the sampling cost $\text{tr}[\rho'_{\text{det}}]^{-2}$ by using QuTiP [33].

Our results are shown in Fig. 3 and Fig. 4. As shown in Fig. 3, we can reduce the infidelity by VQED compared to a single physical qubit without encoding with the same error rate. Furthermore, frequent application of VQED during the circuit execution prevents the noisy state to be highly mixed on the code space. This allows us to suppress logical errors that cannot be mitigated by the conventional SE performed only on the state immediately before the measurement [23, 24]. We also find that we can reduce infidelity without performing error detection after every gate: we can sufficiently mitigate errors simply by performing error detection after every fixed number of gates. This fact can be useful when the measurement time is much longer than the gate execution time. By comparing infidelity among different codes, we can say that infidelity becomes smaller as the code distance gets larger. For the same code distance, the accuracy of calculation depends on how often VQED is performed.

Fig. 4 shows that the sampling cost increases exponentially with the circuit depth L when we perform VQED frequently. This scaling can be roughly considered to be given by the square inverse of the probability

that a state in the code space does not get out of the code space when the noise is applied; thus we can say $\text{tr}[\rho'_{\text{det}}]^{-2} = O((1 - \frac{3}{4}p)^{-2nL})$. On the other hand, when VQED is performed only before the measurement, the sampling cost approaches a constant value. This is because the noisy state approaches the completely mixed state, so the probability of not detecting an error approaches $\text{tr}[I/2^n P] = \frac{1}{2^{n-k}}$.

From the above, we can say that our method can be used effectively by adjusting the code distance or frequency of VQED according to the hardware constraints, the desired accuracy, or the allowable sampling cost.

VI. DISCUSSION

We propose virtual quantum error detection (VQED) so that the computation errors during the circuit execution can be flexibly suppressed by using additional two-qubit operations and measurements in the X basis. We verify in the numerical simulations that our virtual quantum error detection protocol allows for the realization of significantly higher-fidelity calculation of expectation values, compared with the conventional symmetry expansion method, at the cost of sampling costs. We also discuss the virtual implementation of quantum error correction; however, even though the fidelity of the quantum state after quantum error correction is generally lower than that for quantum error detection, the sampling cost of virtual implementation of quantum error correction becomes larger than VQED.

Although we mainly discuss the stabilizer codes based on the Pauli group, we can apply our method to other types of codes such as rotation symmetric bosonic codes (RSBCs) [34] as well. In Ref. [25], symmetry expansion in RSBCs is proposed, but it is restricted to state preparation and immediately before measurement. By considering the rotation symmetry operators rather than Pauli symmetries, we can also perform virtual quantum error detection for RSBCs, which is a significant generalization of Ref. [25]. In this case, we need controlled-rotation gates, which is implemented by the dispersive interactions [35] between the resonator and the ancilla qubit.

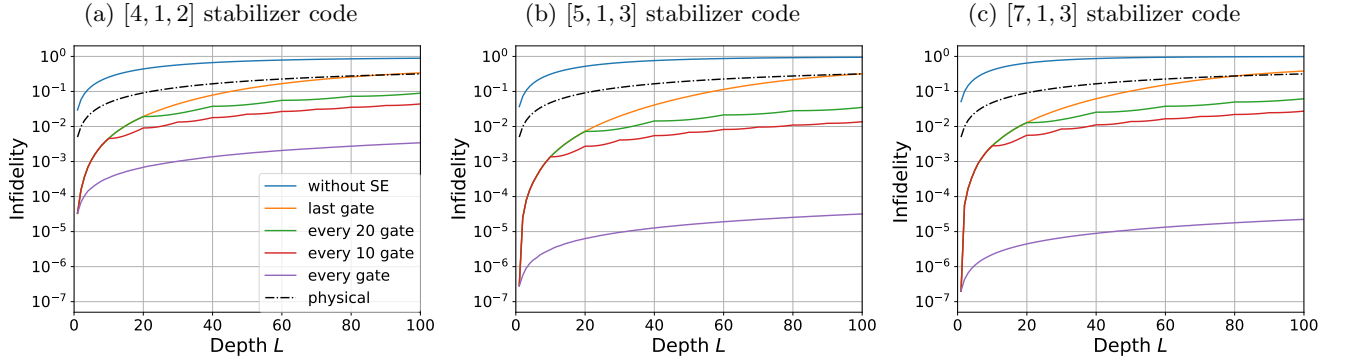


FIG. 3. Depth L dependence of infidelity $1 - \text{tr}[\rho_{\text{det}} |\bar{\Psi}\rangle\langle\bar{\Psi}|] = 1 - \langle\bar{\Psi}|\rho_{\text{det}}|\bar{\Psi}\rangle$ between the output state of the noisy circuit with VQED ρ_{det} and the noiseless circuit $|\bar{\Psi}\rangle$ for (a) $[4, 1, 2]$, (b) $[5, 1, 3]$, and (c) $[7, 1, 3]$ stabilizer codes. The “without SE” line represents infidelity when we did not perform VQED. The “last gate” line represents infidelity when we perform VQED only before the measurement as in Refs. [23, 24]. The “every 20 gates” and the “every 10 gates” lines represent infidelity when we perform VQED after every 20 and 10 gates. The “every gate” line represents infidelity when we perform VQED after every gate. The “physical” line represents the infidelity of a single physical qubit without encoding.

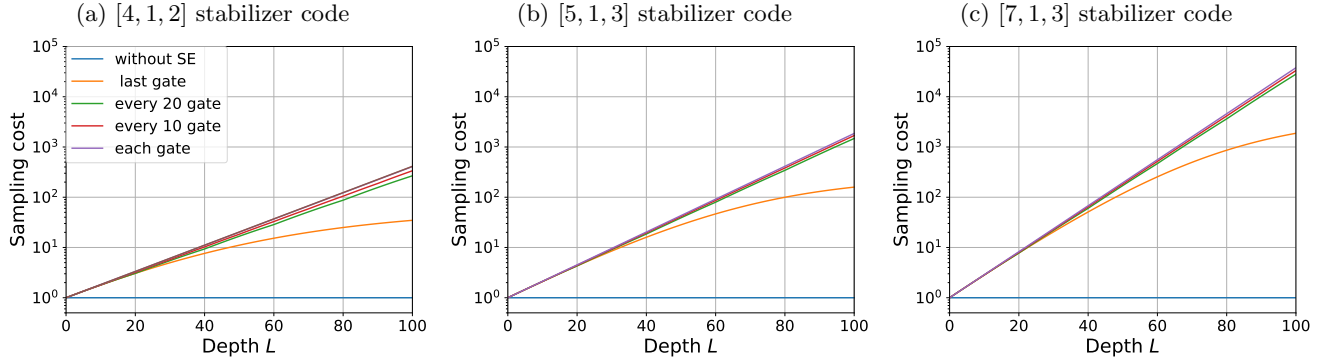


FIG. 4. Scaling of the sampling cost $\text{tr}[\rho'_{\text{det}}]^{-2}$ with respect to the depth L of the quantum circuit for (a) $[4, 1, 2]$, (b) $[5, 1, 3]$, and (c) $[7, 1, 3]$ stabilizer codes. The “without SE” line represents infidelity when we did not perform VQED. The “last gate” line represents infidelity when we perform VQED only before the measurement as in Refs. [23, 24]. The “every 20 gates” and the “every 10 gates” lines represent the sampling cost when we perform VQED after every 20 and 10 gates. The “every gate” line represents the sampling cost when we perform VQED after every gate.

Even after the application of VQED, there remains a finite logical error, e.g., due to the limitations of code distances. Therefore, the efficient combination of VQED with other QEM methods, e.g. purification-based QEM [36–41], will also be an important research direction for the realization of even more accurate quantum computing. Also, because VQED can be regarded as a QEM method implemented on the code space, the relationship between VQED and other hybrid QEM/QEC methods are worth exploring [29, 42–44].

Finally, information-theoretic analysis of QEM is one of the intensively studied topic [45–50]. As far as we know, symmetries of the system is not explicitly considered in these works while our work shows that they can play a crucial role for QEM. Therefore, the construction

of an information-theoretic analysis of QEM incorporating the symmetries may shed light on e.g., the characterization cost of the noise model for performing QEM.

ACKNOWLEDGMENTS

This work is supported by PRESTO, JST, Grant No. JPMJPR1916, JPMJPR2114, JPMJPR2119; CREST, JST, Grant No. JPMJCR1771; MEXT Q-LEAP Grant No. JPMXS0120319794 and JPMXS0118068682, JST Moonshot R&D, Grant No. JPMJMS2061, and COI-NEXT program Grant No. JPMJPF2221. K.T. is supported by Worldleading Innovative Graduate Study Program for Materials Research, Industry, and Technology (MERITWINGS) of the University of Tokyo.

[1] J. Preskill, Quantum **2**, 79 (2018).

[2] S. McArdle, S. Endo, A. Aspuru-Guzik, S. C. Benjamin, and X. Yuan, Reviews of Modern Physics **92**, 015003

- (2020).
- [3] M. Cerezo, A. Arrasmith, R. Babbush, S. C. Benjamin, S. Endo, K. Fujii, J. R. McClean, K. Mitarai, X. Yuan, L. Cincio, *et al.*, *Nature Reviews Physics* **3**, 625 (2021).
 - [4] J. Tilly, H. Chen, S. Cao, D. Picozzi, K. Setia, Y. Li, E. Grant, L. Wossnig, I. Rungger, G. H. Booth, *et al.*, *Physics Reports* **986**, 1 (2022).
 - [5] K. Bharti, A. Cervera-Lierta, T. H. Kyaw, T. Haug, S. Alperin-Lea, A. Anand, M. Degroote, H. Heimonen, J. S. Kottmann, T. Menke, *et al.*, *arXiv preprint arXiv:2101.08448* (2021).
 - [6] F. Arute, K. Arya, R. Babbush, D. Bacon, J. C. Bardin, R. Barends, R. Biswas, S. Boixo, F. G. Brandao, D. A. Buell, *et al.*, *Nature* **574**, 505 (2019).
 - [7] A. Kandala, A. Mezzacapo, K. Temme, M. Takita, M. Brink, J. M. Chow, and J. M. Gambetta, *Nature* **549**, 242 (2017).
 - [8] L. S. Madsen, F. Laudenbach, M. F. Askarani, F. Rortais, T. Vincent, J. F. Bulmer, F. M. Miatto, L. Neuhaus, L. G. Helt, M. J. Collins, *et al.*, *Nature* **606**, 75 (2022).
 - [9] S. J. Devitt, W. J. Munro, and K. Nemoto, *Reports on Progress in Physics* **76**, 076001 (2013).
 - [10] D. A. Lidar and T. A. Brun, *Quantum error correction* (Cambridge university press, 2013).
 - [11] M. Grassl, T. Beth, and T. Pellizzari, *Physical Review A* **56**, 33 (1997).
 - [12] A. M. Steane, *Physical Review Letters* **77**, 793 (1996).
 - [13] P. W. Shor, *Physical review A* **52**, R2493 (1995).
 - [14] R. Laflamme, C. Miquel, J. P. Paz, and W. H. Zurek, *Physical Review Letters* **77**, 198 (1996).
 - [15] R. Hicks, B. Kobrin, C. W. Bauer, and B. Nachman, *Physical Review A* **105**, 012419 (2022).
 - [16] J. M. Günther, F. Tacchino, J. R. Wootton, I. Tavernelli, and P. K. Barkoutsos, *Quantum Science and Technology* **7**, 015009 (2021).
 - [17] K. Temme, S. Bravyi, and J. M. Gambetta, *Physical review letters* **119**, 180509 (2017).
 - [18] Y. Li and S. C. Benjamin, *Physical Review X* **7**, 021050 (2017).
 - [19] S. Endo, S. C. Benjamin, and Y. Li, *Physical Review X* **8**, 031027 (2018).
 - [20] S. Endo, Z. Cai, S. C. Benjamin, and X. Yuan, *Journal of the Physical Society of Japan* **90**, 032001 (2021).
 - [21] Z. Cai, R. Babbush, S. C. Benjamin, S. Endo, W. J. Huggins, Y. Li, J. R. McClean, and T. E. O’Brien, *arXiv preprint arXiv:2210.00921* (2022).
 - [22] X. Bonet-Monroig, R. Sagastizabal, M. Singh, and T. O’Brien, *Physical Review A* **98**, 062339 (2018).
 - [23] J. R. McClean, Z. Jiang, N. C. Rubin, R. Babbush, and H. Neven, *Nature communications* **11**, 1 (2020).
 - [24] Z. Cai, *Quantum* **5**, 548 (2021).
 - [25] S. Endo, Y. Suzuki, K. Tsubouchi, R. Asaoka, K. Yamamoto, Y. Matsuzaki, and Y. Tokunaga, *arXiv preprint arXiv:2211.06164* (2022).
 - [26] S. McArdle, X. Yuan, and S. Benjamin, *Physical review letters* **122**, 180501 (2019).
 - [27] M. A. Nielsen and I. Chuang, “Quantum computation and quantum information,” (2002).
 - [28] D. Gottesman, *Stabilizer codes and quantum error correction* (California Institute of Technology, 1997).
 - [29] Y. Suzuki, S. Endo, K. Fujii, and Y. Tokunaga, *PRX Quantum* **3**, 010345 (2022).
 - [30] L. Lin and Y. Tong, *PRX Quantum* **3**, 010318 (2022).
 - [31] K. Wan, M. Berta, and E. T. Campbell, *Physical Review Letters* **129**, 030503 (2022).
 - [32] R. Zhang, G. Wang, and P. Johnson, *Quantum* **6**, 761 (2022).
 - [33] J. R. Johansson, P. D. Nation, and F. Nori, *Computer Physics Communications* **183**, 1760 (2012).
 - [34] A. L. Grimsmo, J. Combes, and B. Q. Baragiola, *Physical Review X* **10**, 011058 (2020).
 - [35] A. Blais, A. L. Grimsmo, S. M. Girvin, and A. Wallraff, *Reviews of Modern Physics* **93**, 025005 (2021).
 - [36] W. J. Huggins, S. McArdle, T. E. O’Brien, J. Lee, N. C. Rubin, S. Boixo, K. B. Whaley, R. Babbush, and J. R. McClean, *Physical Review X* **11**, 041036 (2021).
 - [37] B. Koczor, *Physical Review X* **11**, 031057 (2021).
 - [38] M. Huo and Y. Li, *Physical Review A* **105**, 022427 (2022).
 - [39] N. Yoshioka, H. Hakoshima, Y. Matsuzaki, Y. Tokunaga, Y. Suzuki, and S. Endo, *Physical Review Letters* **129**, 020502 (2022).
 - [40] A. Seif, Z.-P. Cui, S. Zhou, S. Chen, and L. Jiang, *PRX Quantum* **4**, 010303 (2023).
 - [41] T. E. O’Brien, S. Polla, N. C. Rubin, W. J. Huggins, S. McArdle, S. Boixo, J. R. McClean, and R. Babbush, *PRX Quantum* **2**, 020317 (2021).
 - [42] Y. Xiong, D. Chandra, S. X. Ng, and L. Hanzo, *IEEE Access* **8**, 228967 (2020).
 - [43] C. Piveteau, D. Sutter, S. Bravyi, J. M. Gambetta, and K. Temme, *Physical Review Letters* **127**, 200505 (2021).
 - [44] M. Lostaglio and A. Ciani, *Physical Review Letters* **127**, 200506 (2021).
 - [45] R. Takagi, *Physical Review Research* **3**, 033178 (2021).
 - [46] R. Takagi, S. Endo, S. Minagawa, and M. Gu, *npj Quantum Information* **8**, 114 (2022).
 - [47] R. Takagi, H. Tajima, and M. Gu, *arXiv preprint arXiv:2208.09178* (2022).
 - [48] K. Tsubouchi, T. Sagawa, and N. Yoshioka, *arXiv preprint arXiv:2208.09385* (2022).
 - [49] H. Hakoshima, Y. Matsuzaki, and S. Endo, *Physical Review A* **103**, 012611 (2021).
 - [50] Y. Quek, D. S. França, S. Khatri, J. J. Meyer, and J. Eisert, *arXiv preprint arXiv:2210.11505* (2022).